Quantitative monitoring of brittle fatigue crack growth in railway steel using acoustic emission

Shi, Shengrun; Han, Zhiyuan ; Liu, Zipeng; Vallely, Patrick; Soua, Slim; Kaewunruen, Sakdirat; Papaelias, Mayorkinos

DOI:
10.1177/0954409717711292

Document Version
Peer reviewed version

Citation for published version (Harvard):
Shi, S, Han, Z, Liu, Z, Vallely, P, Soua, S, Kaewunruen, S & Papaelias, M 2018, 'Quantitative monitoring of brittle fatigue crack growth in railway steel using acoustic emission', *Proceedings of the Institution of Mechanical Engineers, Part F: Journal of Rail and Rapid Transit*, vol. 232, no. 4, pp. 1211-1224.
https://doi.org/10.1177/0954409717711292

Quantitative monitoring of brittle fatigue crack growth in railway steel using acoustic emission

Shengrun Shi[a, c], Zhiyuan Han[b], Zipeng Liu[a], Patrick Vallely[a,d], Slim Soua[e], Sakdirat Kaewunruen[f] and Mayorkinos Papaelias[a*]

[a]School of Metallurgy and Materials, The University of Birmingham, UK

[b]Pressure Vessel Department, China Special Equipment Inspection and Research Institute, Beijing China

[c]National Structural Integrity Research Centre, Cambridge, UK

[d]Network Rail, The Mailbox, Birmingham, UK

[e]Integrity Management Group, TWI Ltd, UK

[f]School of Engineering, The University of Birmingham, UK

*Contact author: Dr Mayorkinos Papaelias, M.Papaelias@bham.ac.uk, Telephone: +441214144060

Abstract

Structural degradation of rails will unavoidably take place with time due to cyclic bending stresses, Rolling Contact Fatigue (RCF), impact and environmental degradation. Rail infrastructure managers employ a variety of techniques and equipment to inspect rails. Still tens of rail failures are detected every year on all

major rail networks. Inspection of the rail network is normally carried out at night time, when normal traffic has ceased. As the implementation of the 24-hour railway moves forward to address the increasing demand for rail transport, conventional inspection processes will become more difficult to implement. Therefore, there is an obvious need to gradually replace out-dated inspection methodologies with more efficient Remote Condition Monitoring (RCM) technology. The RCM techniques employed should be able to detect and evaluate defects without causing any reduction in optimum rail infrastructure availability. Acoustic Emission (AE) is a passive RCM technique which can be employed for the quantitative evaluation of the structural integrity of rails. AE sensors can be easily installed on rails in order to monitor structural degradation rate in real time. Therefore, apart from detecting defects AE can be realistically applied to quantify damage. In this study the authors investigated the performance of AE in detecting and quantifying damage in rail steel samples subjected to cyclic fatigue loads during experiments carried out under laboratory conditions. Herewith, the key results obtained are presented together with a detailed discussion of the approach employed in filtering noise sources during data acquisition and subsequent signal processing.

Keywords: Rail defects, cracks, inspection, remote condition monitoring, acoustic emission, quantitative

1. Introduction

In-service rails may develop structural defects due to contact and bending stresses, impact loading and environmental conditions they are subjected to. If defects remain undetected, they will reach critical size resulting ultimately into final failure of the damaged rail section. Therefore, inspection and evaluation of rail damage evolution is crucial for maintenance and track renewal in order to ensure maximum reliability and availability of railway operations.

The growing traffic density coupled with higher axle loads and travel speeds further intensify the need to optimise availability and reliability of rail infrastructure. As network capacity becomes used up by increasing numbers of passengers and freight, financial and mobility consequences arising from unplanned delays and disruption become rapidly amplified. Traditional rail inspection techniques such as Ultrasonic Testing (UT), Magnetic Flux Leakage (MFL) and Eddy Current Testing (ECT) have significant limitations in terms of Probability of Detection (PoD) of certain types of defects and maximum speed of deployment [1-2].

The gradual implementation of the 24-hour railway, already demonstrated by London Underground in the UK, coupled with increasing traffic density further increase the need for effective Remote Condition Monitoring (RCM) of the structural integrity of rails. This is because the time available for inspection using traditional means will gradually drop below to what is required as a minimum to complete the inspection task [1, 3].

More advanced inspection techniques, which have the potential of being deployed under normal train traffic speeds have been investigated extensively, including eddy current pulsed thermography [4-6], Alternating Current Field Measurement (ACFM) [7-13] and pitch-catch ultrasonic testing using EMATs [14]. Although these techniques have yielded promising results, they are more appropriate for the detection of rail head surface breaking defects such RCF cracks. The detection of defects growing in deeper sections of the rail geometry still relies on conventional UT. Although the severity of RCF cracks can be qualitatively assessed using ACFM on the fly, more time-consuming approaches [15] and sophisticated signal processing [16] are required for quantifying damage more accurately. An additional consideration that should be taken into account is that the data gathered from each inspection pass should be correlated with the previous ones in order to establish the rate of propagation of various defects effectively.

Depending on the severity of damage, a defective rail can remain in service with or without repairs being carried out or replaced within a standardised time-schedule ranging from immediately to up to one week after an Emergency Speed Restriction (ESR) has been imposed [17]. For certain defects, the application of fish plates or clamps may be necessary to ensure that, at least theoretically, the defect is not growing further during passage of the trains after the ESR has been imposed. During emergency repairs, normal operation of the railway line affected can be seriously

disrupted resulting in delays and unnecessary costs.

Railway infrastructure managers have been gradually shifting their maintenance strategy from conventional reactive mode to predictive and prognostic modes. In order for predictive and prognostic maintenance approaches to be applied efficiently and reliably in the railway context, identification of the type of defects and evaluation of their severity are necessary. Accurate prediction of the remaining life time of in-service rails would enable better allocation of available resources and improved scheduling of repairs. This would contribute to the overall minimisation of disruption and reduction of cost of maintenance. Moreover, techniques which could confirm the status of in-service rails in terms of whether a defect is propagating or not could allow higher ESRs to be applied instead or the requirement of an ESR to be imposed removed all together [18-20].

AE testing is a dynamic non-destructive testing technique which is extensively used for online Structural Health Monitoring (SHM) and evaluation of critical structural components. AE has the potential of being employed as an efficient tool for real-time monitoring of the structural integrity of rails. The technique is capable of detecting crack growth even at rates as low as 2.5×10^{-6}mm/cycle exhibiting very high sensitivity to small increments of damage [21].

However, an inherent limitation associated with AE is its sensitivity to unwanted

noise sources. Such noise sources include the rubbing of the facets of fatigue cracks or wheel-rail interface interactions associated with friction and/or impact. According to Elber's rule cracks can open and close during loading and unloading cycles. Therefore, the facets of fatigue cracks opening and closing during loading and unloading can rub against each other producing measurable AE events which can be confused with crack growth activity. The rubbing noise can be filtered out as it will occur during the unloading stage of the crack.

To remove the noise arising from fatigue crack facets rubbing various approaches can be applied. For example, one potential approach could be the use of accurate timing parametrisation of the AE measurement. This would ensure that the exact time that the unloading occurs can be pinpointed thus filtering out any AE signals recorded during this period. The unloading event could be established easily using strain gauges in conjunction with the AE sensors.

When the use of strain gauges is not possible or strain measurements are not available, the AE characteristics of the signal can be considered instead. For example, the amplitude, duration, energy and frequency of the AE signals associated with crack facets rubbing against each other will tend to be lower. Hence appropriate thresholds can be applied in order to remove the effect of noise arising from this phenomenon.

To ensure good agreement exists between the AE activity recorded and the actual

structural degradation of the component being monitored, it is highly essential that appropriate filtering and signal processing are employed to discriminate the signals correlated with defects from background noise. AE data filtering and appropriate processing should at least reduce the influence of background noise on the useful part of the signal associated with damage propagation. This is particularly important when AE inspection is performed in a noisy environment like the rail network.

In this study, three-point fatigue crack growth tests have been performed on R260 rail steel samples extracted from the web of a rail section made available by Network Rail. Damage evolution during fatigue tests has been monitored using AE to evaluate the capability of the technique for structural RCM of rails in the field. The analysis of the raw data has been based on the application of different AE signal-related parameters and signal processing based on Spectral Kurtosis (SK). The relationship between Key Parameter Indicators (KPIs) of the AE signal, such as amplitude, AE signal energy and duration, with stress intensity factor (ΔK) have been investigated in order to establish the quantitative relationship between crack growth rate and AE activity detected. The main aim of this study has been to identify the core principles of the AE data analysis required to be carried out to both detect and quantify crack growth events in rail steel.

Although the relationship of certain KPIs with ΔK has been reported previously for various steel grades, including rail steel, as a means of predicting fatigue life and

crack length [22-27] none of them has considered the effect of loading frequency, and the relationship of AE duration rate (dd/dn) with ΔK as an alternative to AE energy rate (de/dn) which has conventionally been employed in the past. Also complete waveform analysis using SK is reported for the first time.

There are various signal processing techniques that can be applied for the analysis of waveforms captured during AE testing. These include both time and frequency domain analysis such as moving RMS, Crest Factor and Kurtosis (time-domain) and Fast Fourier Transform (FFT), spectral subtraction, correlation, etc. (frequency domain). The use of SK is advantageous because it enables the simultaneous analysis of the AE waveforms in both time and frequency domains. Nonetheless, further work not reported herewith has been ongoing to investigate the appropriateness and effectiveness of alternative signal processing techniques, including the use of wavelets.

Railway steel grades have a predominantly pearlitic microstructure. Pearlite tends to behave differently during fatigue crack growth in comparison with steel grades with a ferritic microstructure due to the presence of the harder cementite (Fe_3C) lamellae. This gives also rise to different AE response characteristics. Bassim et al., Yilmazer, and Han et al. have investigated AE monitoring of crack propagation in rail steel [19, 25-27]. However, the relationship between AE signals and fatigue crack growth in rail steel is yet to be evaluated in depth and subsequently under actual operational

conditions. The present study has focused on establishing the necessary criteria that need to be applied during AE testing for data acquisition and subsequent signal processing so as effective quantification of damage propagation can be realised. Although the results of this work are based on laboratory experiments the principles are similar to those applicable in the field.

2. Rail defects

Rail steel cleanliness has improved profoundly in recent decades. Therefore, the occurrence of rail failure due to manufacturing defects is unlikely [1, 28]. The quality of newly produced rails is also checked prior to installation on the network using various non-destructive evaluation (NDE) techniques including UT, ECT and MFL which further reduces the likelihood of manufacturing-related failures [1].

Defects caused by improper usage, handling or installation of a rail section can occur but they are also not common. In most cases defects detected in rails have arisen due to structural degradation from loads sustained with time. In-service, rails are subjected to five major types of stresses, including bending, shear, contact, thermal and residual stresses. Bending and contact stresses are the most significant in terms of their cumulative fatigue damage effect.

Due to the superior hardness of R260 steel grade, wear of the rail head is limited. This however, gives sufficient time for surface and near-surface defects to initiate with

time due to Rolling Contact Fatigue (RCF) [29-30]. Other types of rail defects commonly encountered include transverse and longitudinal cracks in the rail head, bolt hole cracking, vertical cracking or more rarely rail foot corrosion [28]. Any of these defects, if it remains undetected will grow to critical dimensions eventually resulting in final failure of the damaged rail section.

The rail industry employs a Rail Defect Management (RDM) system for reporting and monitoring and archiving rail failures. Rail failure reports can subsequently be used to build a general statistical picture of the occurrence of rail failures, their causative factors and their frequency within the rail network [1, 28]. This information can then be used to evaluate the inspection requirements for a particular section of the rail network. RDM systems could in the future become integral parts of the implementation of rail RCM based on AE.

3. Remote Condition Monitoring using Acoustic Emission

A distinct advantage of AE over conventional NDE techniques is that it is passive in nature. Hence ultrasonic piezoelectric transducers can be used to capture the elastic energy released in the form of stress waves as damage evolves in a solid. AE activity can arise from various sources in a structural material including dislocation slip, micro-cracking initiation and subsequent growth, impact, phase transformation, corrosion, fibre breaking, debonding and delamination [31]. Detection of a growing

defect does not require the sensor to be installed over it since stress waves from the source will propagate for some distance. Gradual attenuation of the propagating stress waves will take place as distance between the source and the sensor increases. The level of attenuation is not the same in every material and will depend on several factors including its Young's modulus and microstructural characteristics, such as grain size, phase constituents, presence of voids, anisotropy, etc. However, since AE is passive in nature, quantification of defect size is inherently more difficult. Individual AE signals need to be correlated between them and overall AE activity trended using various KPIs in order to evaluate damage severity.

One significant drawback of the AE technique, is the fact that it is only sensitive to active damage. If a defect is no longer growing, then no AE activity will arise from it and hence no signals will be logged. Nonetheless, in the case where several defects are present in the structure, growing defects will generate AE activity. Individual AE sources can be distinguished using various location techniques. Linear location is the simplest approach and requires the use of two AE sensors. This location technique is appropriate for use when damage is evolving somewhere between the two AE sensors. In more complex situations zonal or point location techniques are normally required involving at least three AE sensors or more.

In in-service rails AE activity is expected to be generated when the rails are loaded, hence when rolling stock is moving over them. AE signals may arise due to

mechanical noise from wheel-rail interaction, wheel tread damage such as flats giving rise to impact noise, faulty axle bearings, braking, tension and compression due to thermal dilation and contraction, fatigue crack growth and corrosion. Fatigue crack growth in rails will only occur when rolling stock loads the rail. Therefore, although the principles of AE testing require that the structure is continuously monitored for fatigue crack growth related events, in the case of rails this will only occur when sufficiently high loads are applied on the rail section being monitored by passing rolling stock. Hence, AE data logging can be reduced to a few seconds per loading sequence, i.e. only when rolling stock is passing over the instrumented rail section.

AE signals can be classified into two types of waveforms; continuous and burst-type (shown in figure 1). During fatigue crack growth burst-type signals are expected. Continuous signals are likely to arise due to mechanical noise and will have different characteristics. However, rubbing fatigue crack facets can also produce burst type AE signals and therefore appropriate filtering needs to be carried out to remove them as discussed earlier in the present paper.

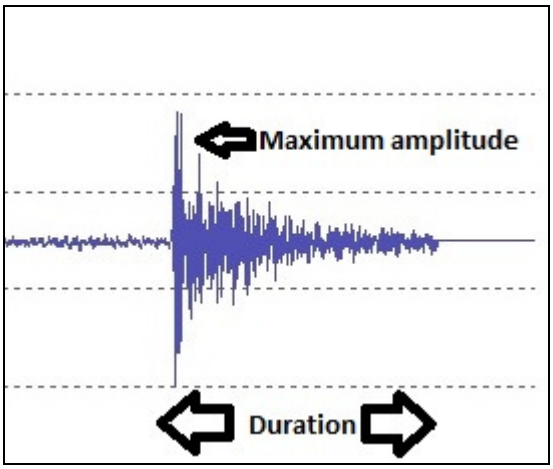

Figure 1: Burst-type AE signal arising from a crack growth event.

AE acquisition can be based on the use of preset parameters or signal (complete waveform) logging. In parameter-based acquisition only signals that fulfill the characteristics of the parameters set are logged. In signal-based acquisition the entire signal is captured over the preset period of time. Both techniques have advantages and disadvantages. Parameter-based acquisition requires the detection of important events only, such as crack increments, in the entire AE activity occurring over time. The rest of the signal not associated with an important event is discarded. In signal-based acquisition the entire waveform is logged over time. Subsequent analysis needs to be carried out to evaluate the signal features associated with damage propagation.

The sampling rates employed in AE testing are normally in excess of 1MS/s. This means that signal-based acquisition can only be maintained over a few tens of seconds at best before data processing becomes very computationally demanding. Also the data files created are much larger in size in comparison with parameter-based files which contain the signal only from the event of interest. Capturing the entire waveform offers the opportunity of more in-depth signal processing but logging needs to be interrupted after a few tens of seconds of acquisition at high sampling rates. Parameter-based logging can be maintained for very long periods of time as long as events of interest are not excessive in number resulting in very high number of AE hits being recorded. For rail RCM, AE signal-based acquisition is possible since

loading will only occur over a few seconds; for as long as the rolling stock needs to pass over the instrumented rail section. The signal-to noise ratio can be easily evaluated from the captured waveform.

In order to analyse the complete AE waveform various signal processing techniques can be employed. Signal analysis can be carried out in the time, frequency or time-frequency domain. Time domain analysis can be carried out by processing the waveform with respect to peak-peak values, moving RMS, Crest Factor and Kurtosis. Frequency domain analysis on the other hand can be based on the application of Fast Fourier Transform (FFT) to extract the power spectrum of the raw signal, spectral subtraction, wavelet analysis or signal correlation. Alternatively, FFT can be applied on the envelope of the demodulated signal. SK is particularly useful for characterizing signal transients and their location in the time and frequency domains. SK was originally introduced by Dwyer as the normalized fourth moment of the real part of short time fourier transformation (STFT) [32]. Otonnello and Pagnan modified the original definition and defined SK as the fourth order moment of the magnitude of STFT [33-34]. Antoni proposed Equation 1 for calculating the SK [35]:

$$K_y(f)=S_{4y}(f)/[S_{2Y}(f)]^2-2 \qquad (1)$$

$$\text{and } S_{nY}(f) \triangleq \langle \, | \, Yw(t,f) \, |^n \rangle$$

$$Yw(t,f) \triangleq \sum_{-\infty}^{\infty} Y(n) * W(n-t)e^{-j2\pi nf}$$

where Yw(t,f) is estimated using STFT and Y(n) is the selected part of the signal Y(t) using and W(n) is the window function which is zero-valued outside the chosen interval. The most important parameter in designing a SK estimator is the selection of the window size. If the window size is set too big, the SK value will decrease very quickly after a certain limit is exceeded, whereas if it is set too small, some bias will be induced.

The stress waves emitted from a source can propagate towards the sensors in different types of waves (compression and shear waves, Rayleigh (or surface) waves and Lamb waves) and modes (longitudinal, flexural and torsional). The type of waves transmitted to the sensor will depend on the geometry of the structure as well as the distance between the source and the sensor.

4. Test rail steel grade and fatigue specimen extraction

The R260 rail steel grade has become the most widely used steel grade for rail manufacturing worldwide. It has a predominantly pearlitic microstructure with very small amounts (>1%) of pro-eutectoid ferrite present along the pearlite grain boundary. The chemical composition and material properties for the R260 steel grade are summarised in Tables 1 and 2 respectively [36].

Table 1: Typical chemical composition of R260 steel grade (in weight %) [36].

C	Si	Mn	P	S	Cr	V	Al	N
0.6-0.82	0.13-0.6	0.65-1.25	<0.03	0.008-0.03	<0.15	<0.03	<0.004	<0.008

Table 2: Typical mechanical properties of R260 rail steel grade [36].

Minimum UTS(ultimate tensile strength)/MPa	Minimum elongation / %	Hardness / BHN
880	10	220-260

Standard single edge notched specimens were extracted from new (three samples) and used (one sample) R260 steel grade rail sections provided by Network Rail with dimensions 120mm x 20mm x 10mm. As it can be seen from figure 2, all fatigue specimens were extracted from the web plane, in the longitudinal orientation of the rail steel.

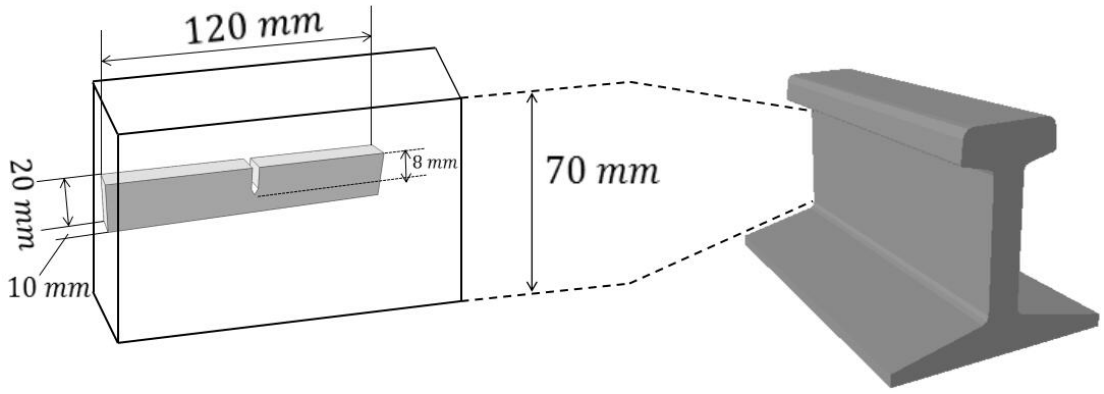

Figure 2: Schematic showing the location on the rail section from which the fatigue specimens were extracted.

The optical micrograph in figure 3 shows the typical pearlitic microstructure of R260 steel grade. The presence of small amounts pro-eutectoid ferrite is visible in some areas along the pearlite grain boundaries.

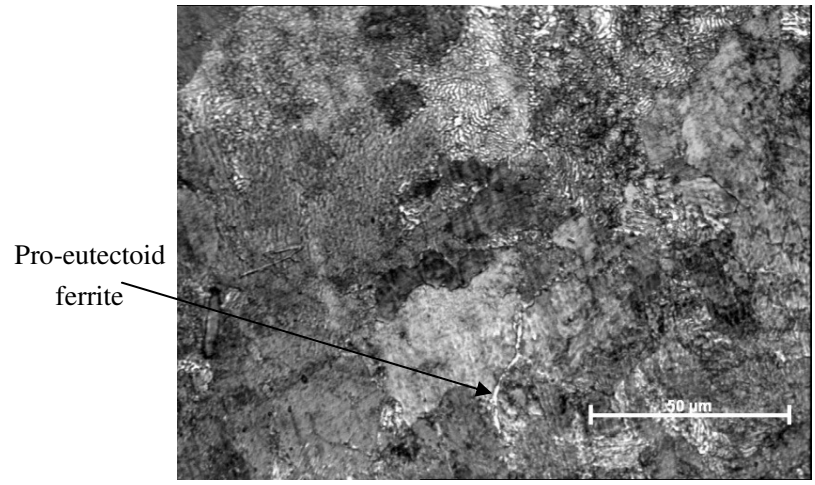

Figure 3: Optical micrograph of R260 steel grade showing a predominantly pearlitic microstructure. Some very small amount of pro-eutectoid ferrite can be seen at the grain boundaries in some areas.

5. Experimental procedure

Three-point bending fatigue testing is partially representative of the type of loading experienced by rails supported by two sleepers underneath it. Although, rail stresses at the wheel-rail interface involve RCF loads, certain defects, such as vertical cracks in the web or foot of the rail, will grow due to bending stresses only. Therefore, the laboratory three-point bending fatigue testing carried out in this study fulfils certain important real-life loading criteria for rails installed on the network.

The three-point bending fatigue tests were performed using a Dartec 50kN servo-hydraulic universal test machine. All tests were carried out at room temperature. The three specimens extracted from the new rail section were pre-cracked using a Vibrophore to initial crack lengths of 9.5mm, 10mm, and 10.8mm respectively. All specimens were tested under sinusoidal cyclic loading at a frequency of 1Hz and load ratio, R = 0.1.

One additional three-point bending sample was extracted from the web of a used rail section removed from the UK rail network. This sample had the same geometrical dimensions as the other three samples but the notch depth was kept to only 2mm with 30° angle. The last fatigue sample was also pre-cracked using a Vibrophore to an initial crack length of 3mm. This sample was also tested under sinuisoidal cyclic loading but at a frequency of 10Hz and load ratio, R = 0.1 using an ESH servo-hydraulic universal testing machine.

For the first three specimens the peak load was set at 3.5kN. For the sample extracted from the used rail section the peak load was set at 9kN. The fatigue crack length was measured throughout the fatigue process using a Direct Current Potential Drop (DCPD) instrument calibrated with respect to the original notch depth. The actual crack lengths with respect to ΔK were calculated for all samples following testing completion. The fractured surfaces of the tested specimens were observed using a Scanning Electron Microscope (SEM).

AE signals generated during the fatigue tests were recorded and analysed using a commercial industrial AE system procured by Physical Acoustic Corporation, PAC, (now Mistras), U.S.A. Two Pico wideband AE piezoelectric transducers with a bandwidth range between 150-750kHz were used to monitor AE activity during fatigue testing of the first three samples. Two PAC R50A narrow band resonant sensors with an operating frequency of 150–700kHZ were employed for the test of the fourth sample. The pico AE sensors were coupled to the surface of the sample using vaseline and held in place with duct tape. The R50A sensors were coupled to the surface of the fourth sample using Araldite®.

The AE sensors were mounted approximately 20mm away from the centre of the sample, one on either side of the cracked region. The signals from the AE sensors were amplified using PAC pre-amplifiers set at 40dB gain. The main amplification stage was set at 6dB provided together with the phantom voltage of 28V by a PAC DiSP acquisition board. AE data were logged using the PAC AEwin v2 software package.

During AE signal acquisition for the first three samples, a signal filter of 100–1000kHz was employed to minimise the effect of unwanted mechanical noise during fatigue testing. The AE minimum amplitude and duration thresholds were set at 40 dB and 50 μs respectively. For the fourth sample, due to the noisier testing

configuration arising from the more rapid cyclic loading (10Hz), the filtering range employed was set slightly higher at 200–1000kHz. Also the amplitude threshold was set at 55dB. The sampling rate in all cases was set at 2MS/s.

6. AE results and analysis

Fatigue crack growth in all four samples was successfully monitored using the AE technique. The scatter observed in the total fatigue lifetime recorded for each sample is attributed to the different pre-crack lengths achieved prior to the actual three-point fatigue bending tests. In figure 4a-h crack growth has been plotted with respect to AE signal amplitude and duration with number of fatigue cycles for each of the tested specimens. Once a critical crack length was reached all samples failed in brittle fashion as shown in figure 5.

For the first three specimens the critical crack length was determined to be near 13mm. At this point ΔK became too high resulting in final brittle failure of the specimens. The fourth sample also failed in brittle fashion once the critical crack length of approximately 5.2mm was reached. Small sudden increments in crack growth did occur during fatigue testing of all samples. Such increments were very clearly obvious in the fourth fatigue sample extracted from the used rail section.

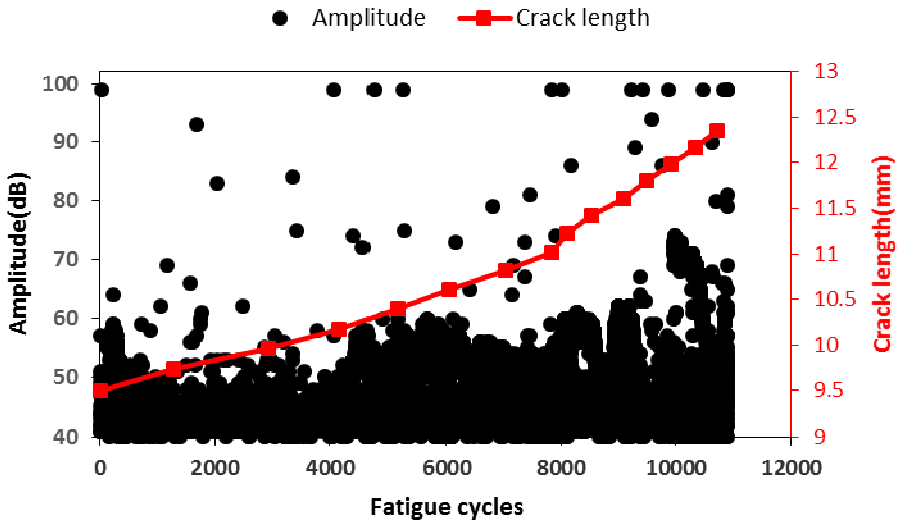

a) Specimen A – AE signal amplitude in dB versus number of fatigue cycles with crack growth in mm

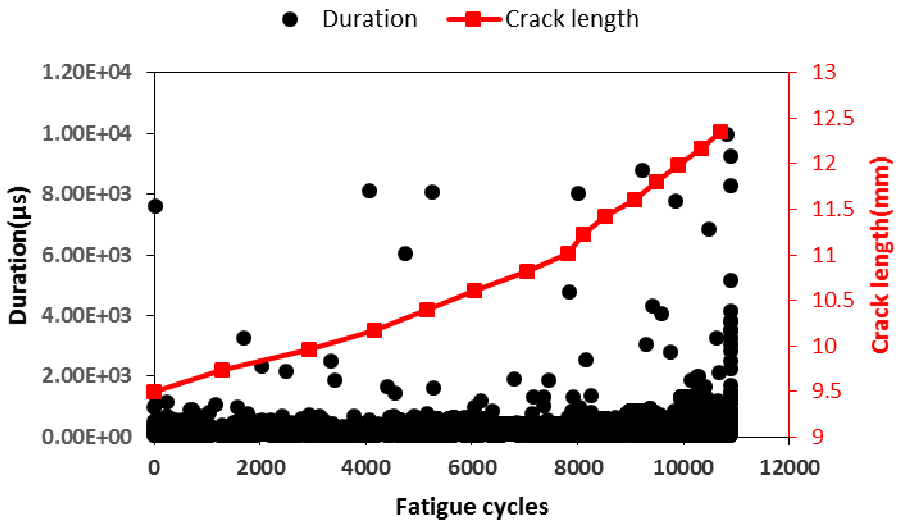

b) Specimen A – AE signal duration in µs versus number of fatigue cycles with crack growth in mm

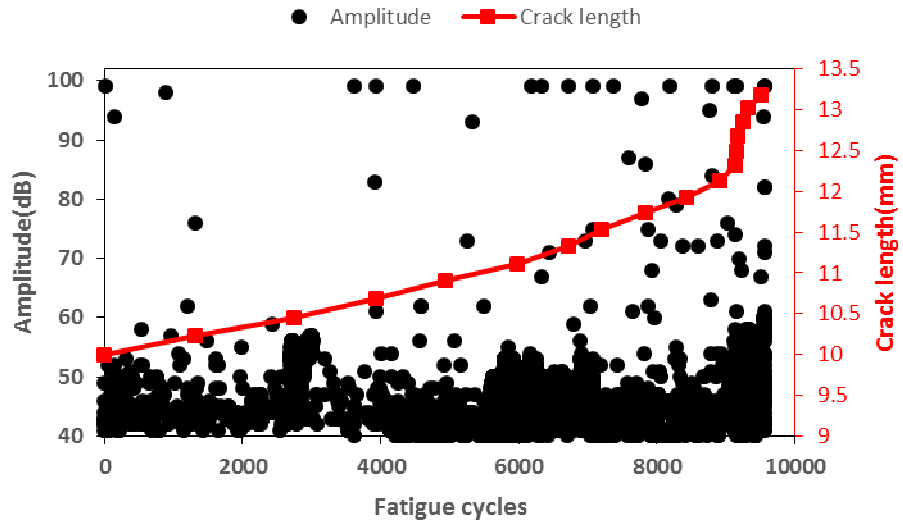

c) Specimen B – AE signal amplitude in dB versus number of fatigue cycles with crack growth in mm

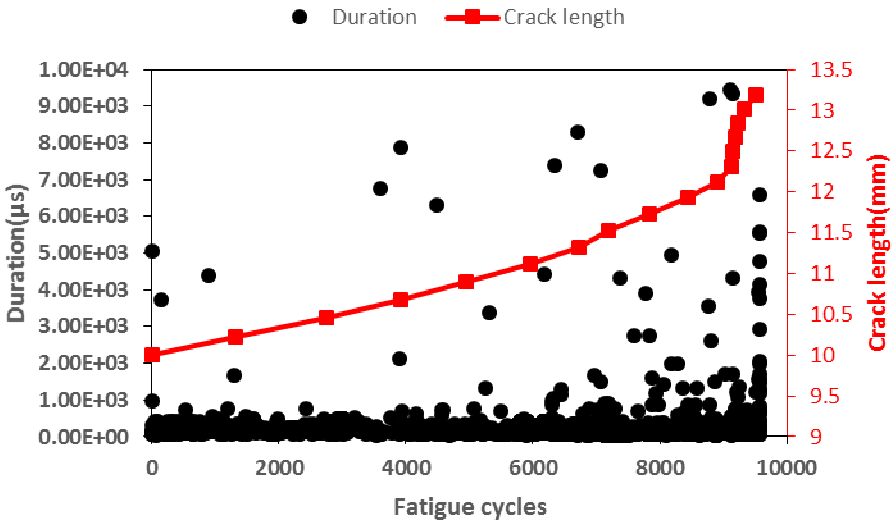

d) Specimen B – AE signal duration in µs versus number of fatigue cycles with crack growth in mm

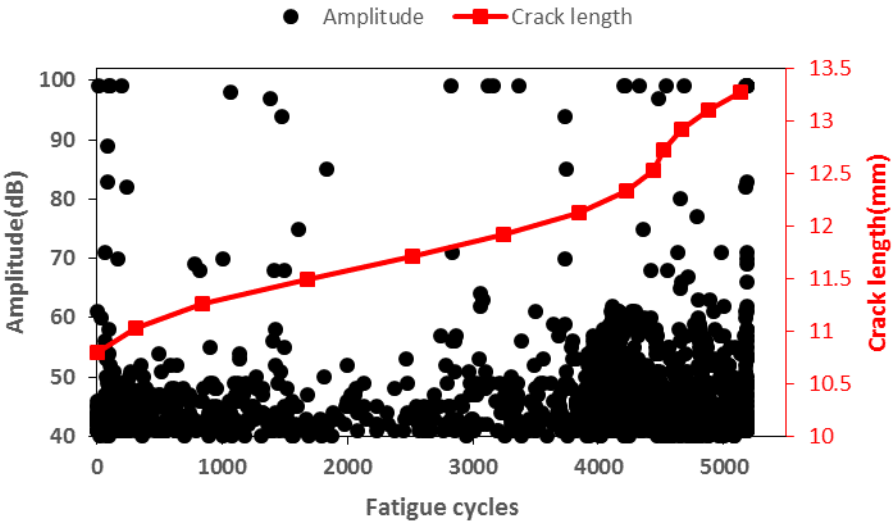

e) Specimen C – AE signal amplitude in dB versus number of fatigue cycles with crack growth in mm

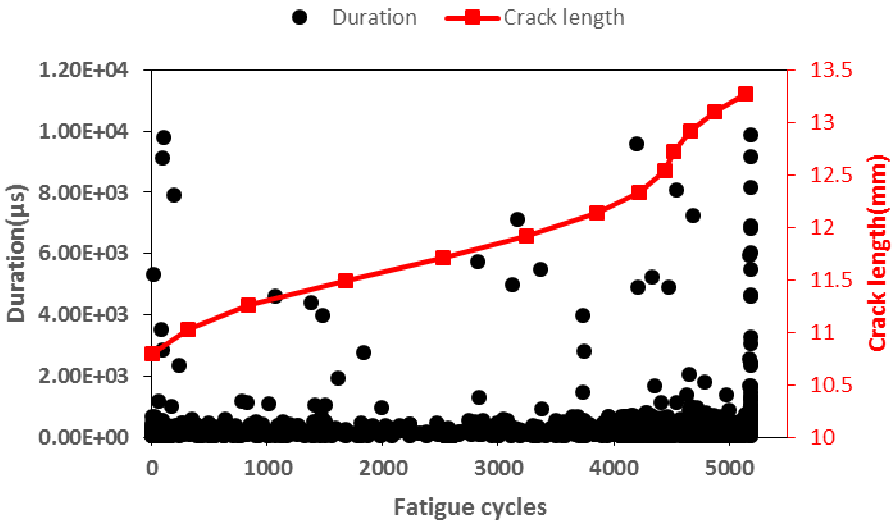

f) Specimen C: AE signal duration in µs versus number of fatigue cycles with crack growth in mm

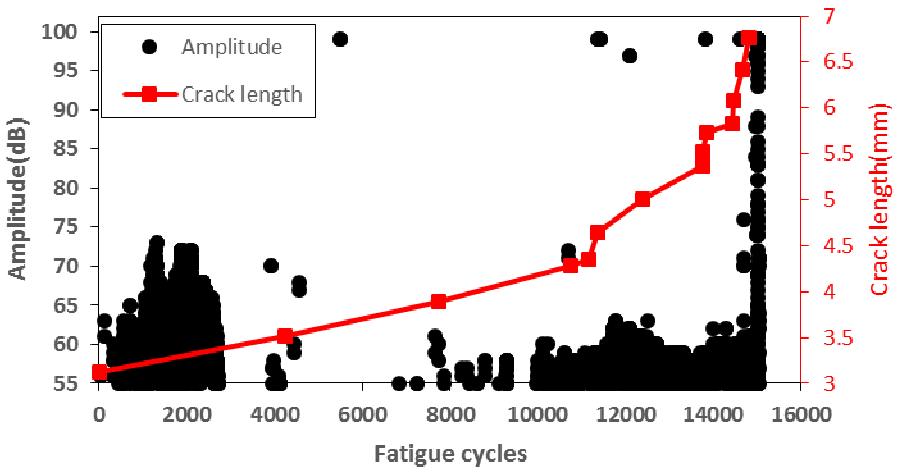

g) Specimen D: AE signal amplitude in dB versus number of fatigue cycles with crack growth in mm

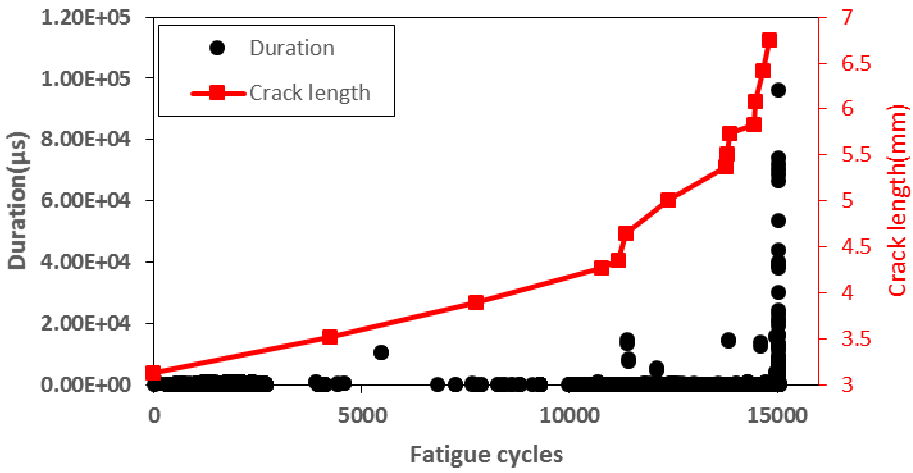

h) Specimen D: AE signal duration in µs versus number of fatigue cycles with crack growth in mm

Figure 4: a-h) AE signal amplitude and duration plots versus number of fatigue cycles with crack growth.

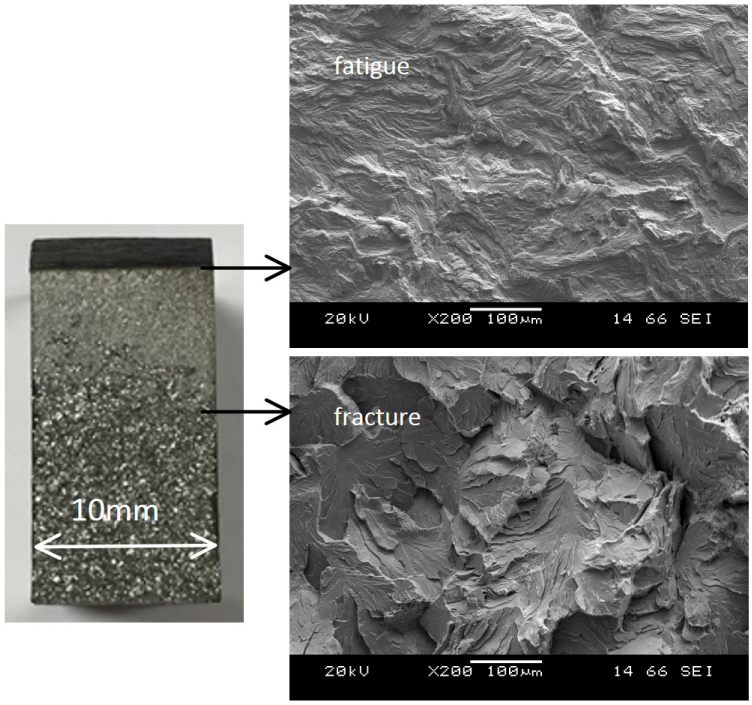

Figure 5: Macroscopic view of the fractured surface of one of the fatigue samples with SEM micrographs showing the morphologies of the fatigue crack growth area and the brittle fracture area.

For all samples with the exception of the fourth sample, high amplitude AE events were detected throughout the duration of the fatigue test. The discrepancy in the fourth sample could be related to the different sensor and filtering employed. It is evident that the longer duration AE events recorded are predominantly related to those exhibiting also high signal amplitude. As crack length extends nearer to critical dimensions and final failure becomes imminent a higher population of high amplitude and high duration AE events are recorded. In fact, the longer duration AE signals are recorded just prior and during the final failure stage of the sample. The same trend is exhibited by all samples tested.

An interesting feature in plots 4g-h is the quiet stage in AE activity during testing of the fourth sample. During this stage only a few AE events are recorded due to the fact that crack growth is still very small. The intense activity recorded prior to any crack growth is attributed to dislocation movement and plasticity in the crack tip zone. AE activity does intensify gradually as crack grows.

Some high amplitude and high duration AE events are detected during momentary accelerations in crack growth rate. Such events have been clearly captured by the DCPD measurements as well as the AE instrument. By plotting the cumulative AE energy it is evident that the AE activity detected closely matches the DCPD measurement. The plots in figures 6 and 7, show the measured crack length using DCPD and the cumulative AE energy for the fourth sample respectively. The plot in figure 8 is the zoomed in part of the signal.

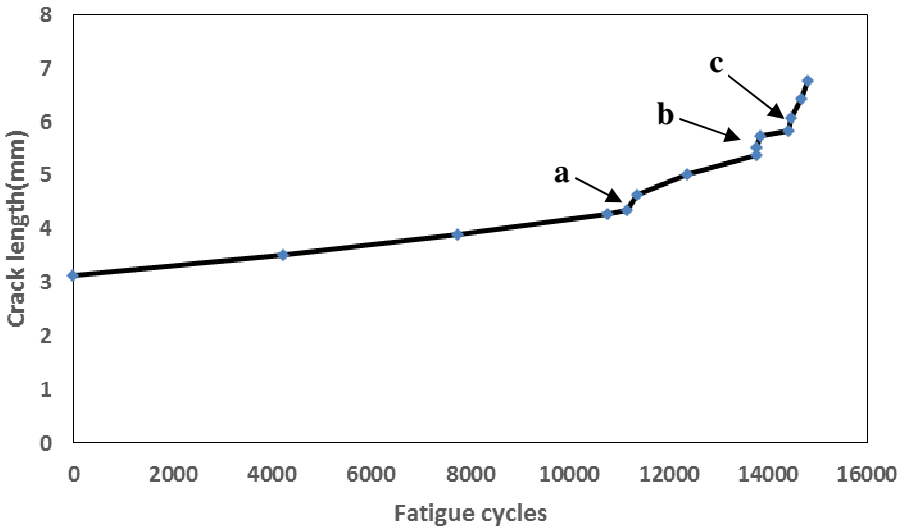

Figure 6: Crack growth length measured with DCPD versus testing time. Points a, b

and c indicate the points where crack propagation exhibited momentary acceleration.

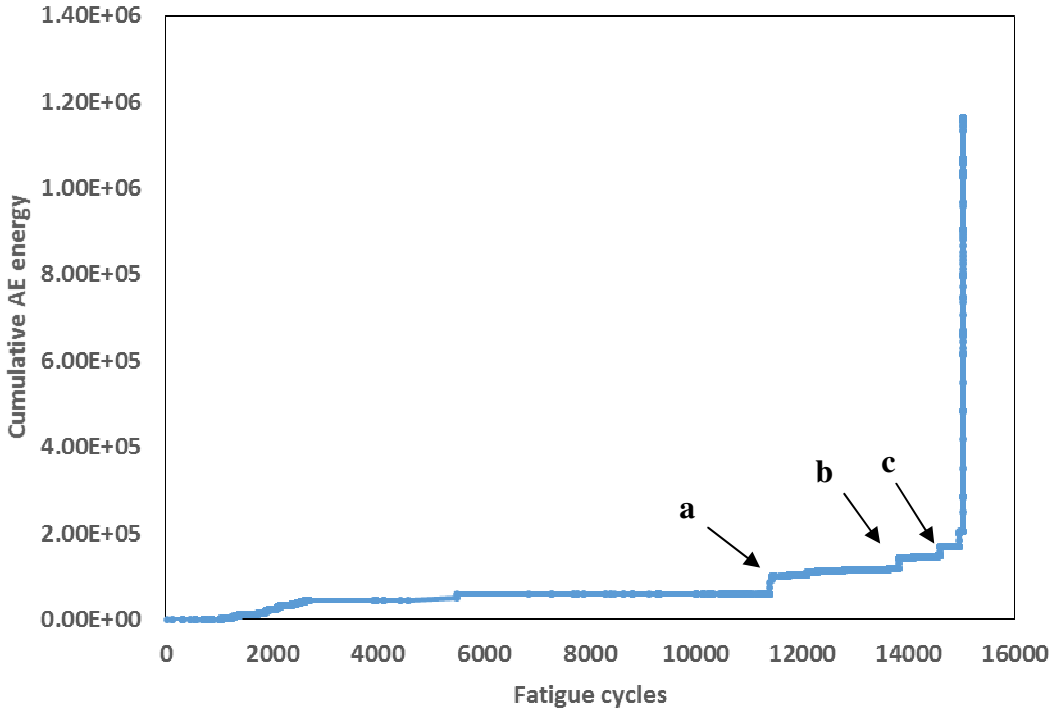

Figure 7: Plot of cumulative AE energy with number of fatigue cycles for the fourth sample. The points where crack growth rate has accelerated are also marked by a clear sudden increase in the accummulated AE energy

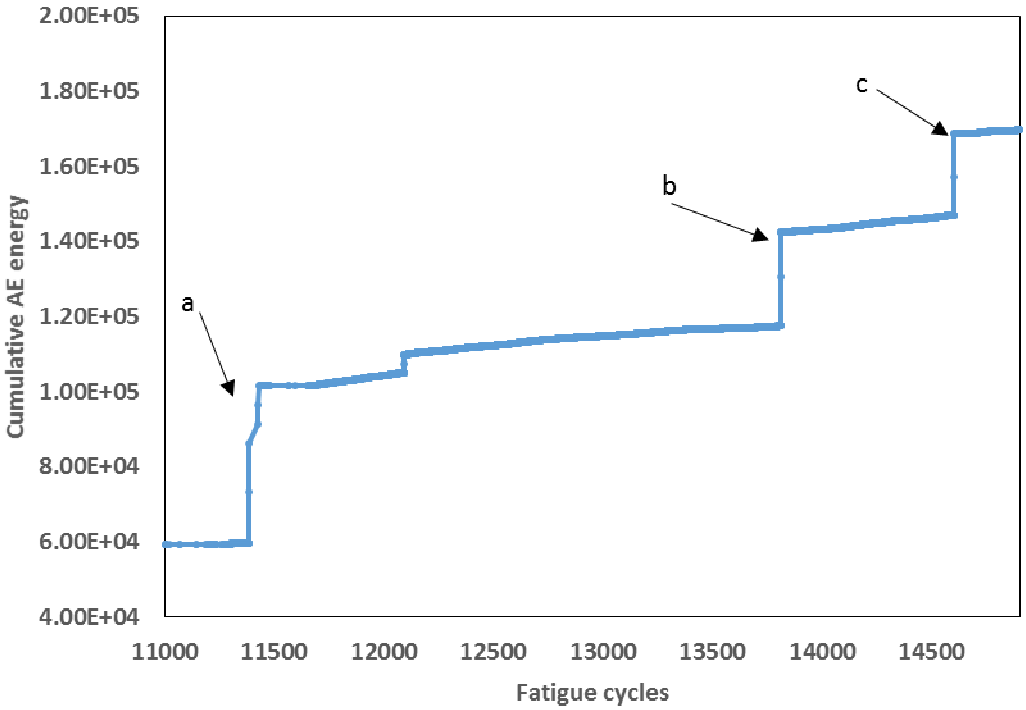

Figure 8: Zoomed in part of the cumulative AE energy with number of fatigue cycles. The sudden increase in the accummulated AE energy is more clearly manifestated. This is due to the fact that significant AE energy is emitted at the final stage of structural failure of the sample.

Subsequent microscopic analysis of the fractured surface of the fourth sample revealed the locations where crack growth accelerated momentarily during testing. This is shown in the micrographs in figure 9. It is evident that the morphology changes sharply from smooth (fatigue morphology) to cleavage (fracture morphology) when the crack growth accelerated. The exact locations where cleavage facets have been found correspond well in terms of crack depth measured and AE activity recorded in test time.

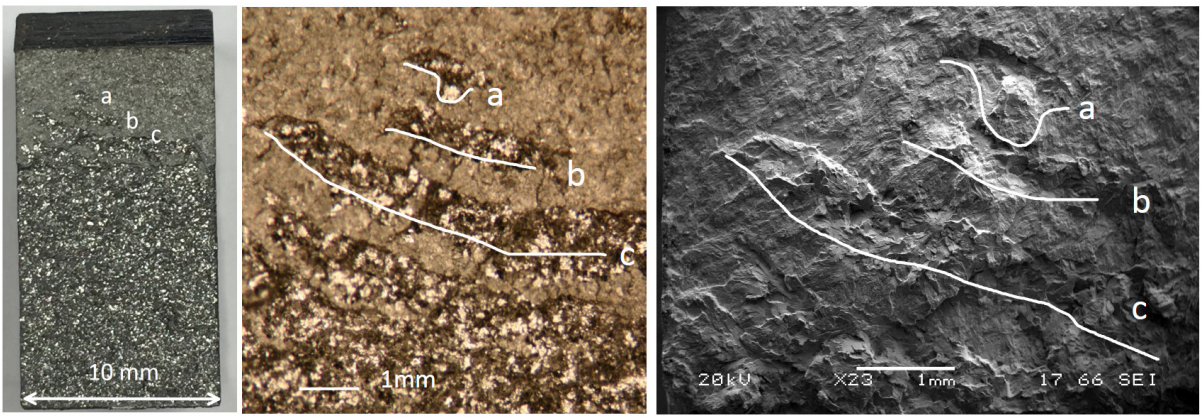

Figure 9: The fractured surface of the fourth specimen showing evidence of cleavage fracture at the locations where the AE energy accumulation rapidly increased and where a sudden acceleration in crack growth rate was recorded by the DCPD instrument.

Previous research has shown that AE energy and energy rate can be used for quantitative analysis of the AE data. However, AE duration rate has not been considered previously. Since the energy of the AE signal is directly related to the duration and amplitude, AE energy rate and duration rate are expected to follow similar trends. Figure 9 shows the fatigue crack growth rates (da/dN) and AE energy rates (dE/dN) with ΔK on the double logarithmic axes. Figure 10 shows the fatigue crack growth rates with AE duration rate (dD/dN). The similarities between the two plots are obvious indicating there is a close relationship between the two parameters. For all samples the Paris-Erdogan law is obeyed [37]:

$$\frac{da}{dN} = C\Delta K^m \text{, or: } \log(\frac{da}{dN}) = \log C + m\log\Delta K \quad (2)$$

where C and m are constants for a particular material. The fitting values for the first 3 samples are summarised in Table 3.

Since dE/dN exhibits similar trend as da/dN, the relationship between dE/dN and ΔK can be described as [37-38]:

$$\frac{dE}{dN} = B\Delta K^{p}, \text{ or: } \log(\frac{dE}{dN}) = \log B + p\log\Delta K \tag{3}$$

The fitting parameters (C, m, B, and p) are also summarised in table 3.

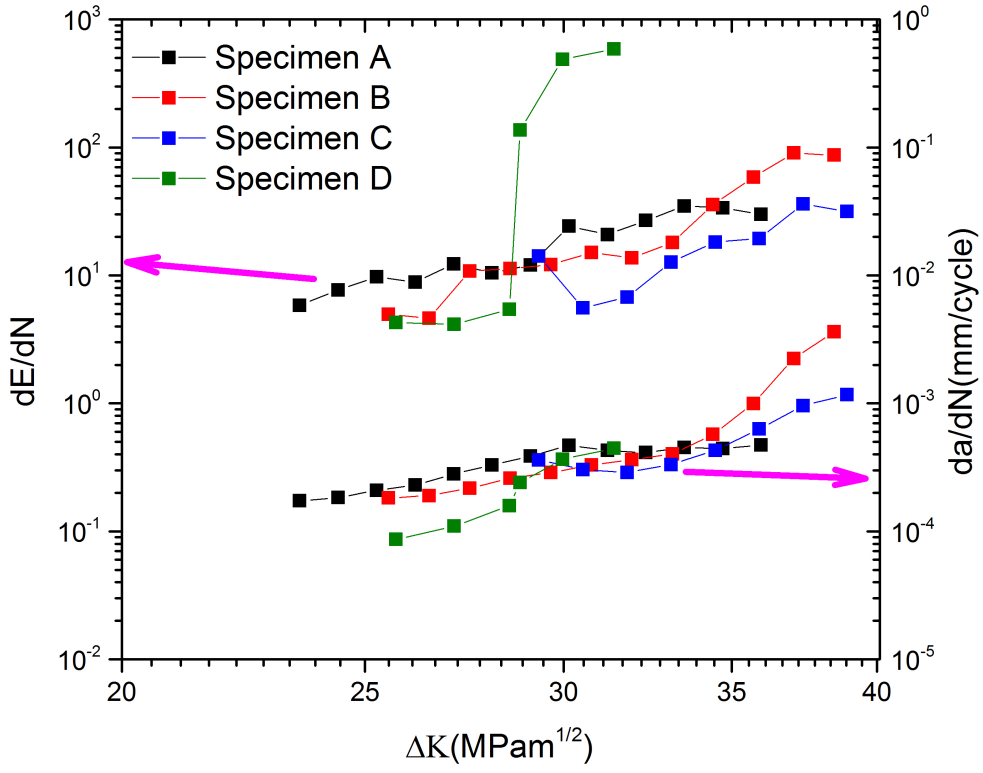

Figure 9: da/dN and dE/dN with ΔK for all four samples. The fourth sample exhibits large excursion due to momentary acceleration of crack growth at certain stage.

Despite the fact that all four samples largely obey the Paris-Erdogan law dE/dN does exhibit fluctuations which are particularly evident in samples C and D. Similar results are yielded when plotting dD/DN with ΔK.

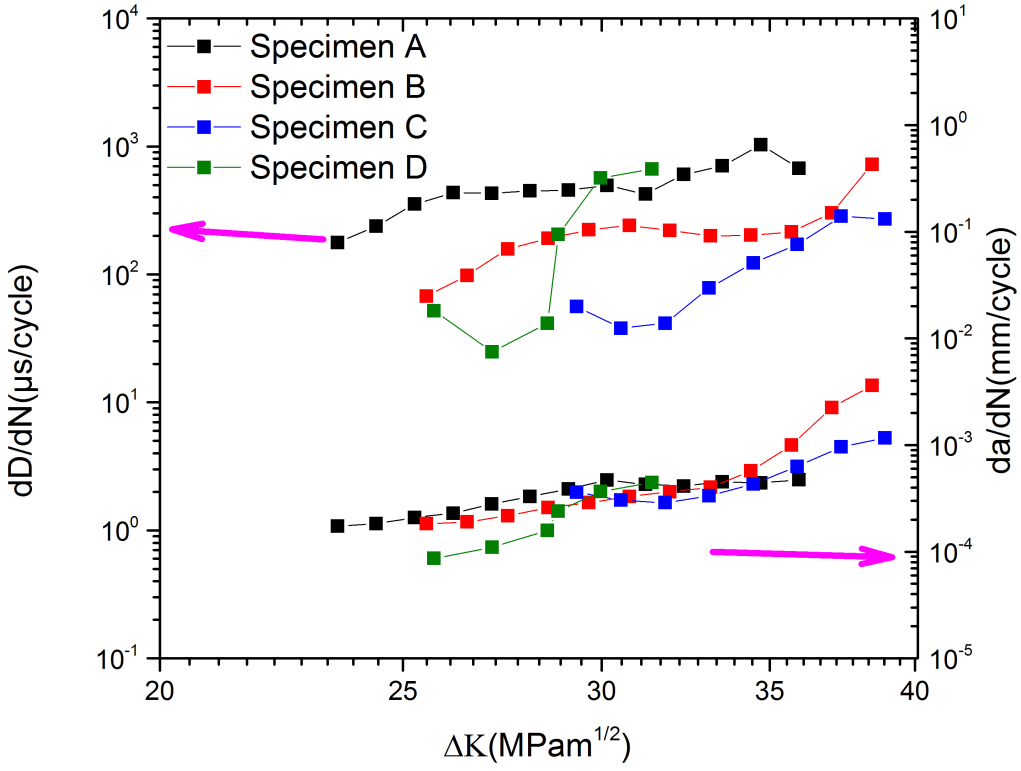

Figure 10: Crack growth rate and duration rate with ΔK. The results for dD/dN with ΔK show similar trends with those for dE/DN.

From the results obtained it is apparent that prediction of rail steel fatigue lifetime using AE is not straightforward and requires further investigation. This is attributed to cleavage fracture which results in high amplitude, high duration and hence high energy AE events as it was clearly shown for the fourth sample. Brittle fracture events

appear to occur intermittently throughout the fatigue crack growth process. However, for the fourth sample these events seem to intensify as the crack length nears critical dimensions.

Table 3: Summary of pre-crack length and total loading cycles to failure for the first three samples tested at 1Hz.

Sample	**Pre-crack length in mm**	**Total loading cycles to failure**	**M**	**C**	**P**	**B**
A	9.5	10894	6.07	5E-13	4.29	8E-06
B	10	9579	6.65	5E-14	7.23	3E-10
C	10.8	5196	4.88	2E-11	5.45	7E-08

7. Signal-based acquisition and analysis

One additional sample was pre-cracked and subjected to 1Hz sinusoidal cyclic loading using the DARTEC servo-hydraulic universal testing machine. The purpose of these tests was to evaluate the complete AE waveform with and without crack propagation occurring. AE activity was monitored using a PAC R50A sensor connected to a customised AE system which was set to acquire for 5s intervals every 10s. The sampling rate was set at 1MS/s. Pre-amplification and amplification stages were held the same as before (40dB and 6dB respectively). No previous filtering has been applied to the acquired signal.

Prior to testing the pre-cracked rail steel specimen, a reference mild steel sample without any notch or cracking was used to evaluate the background noise level and AE waveform arising under this particular testing configuration. Figure 11 shows the raw AE signal captured for the reference sample. As it can be seen the peak to peak value is very low and there are no distinct peaks indicating the presence of any crack growth. The small fluctuations in the signal are due to mechanical noise from the hydraulic pump during loading and unloading of the sample.

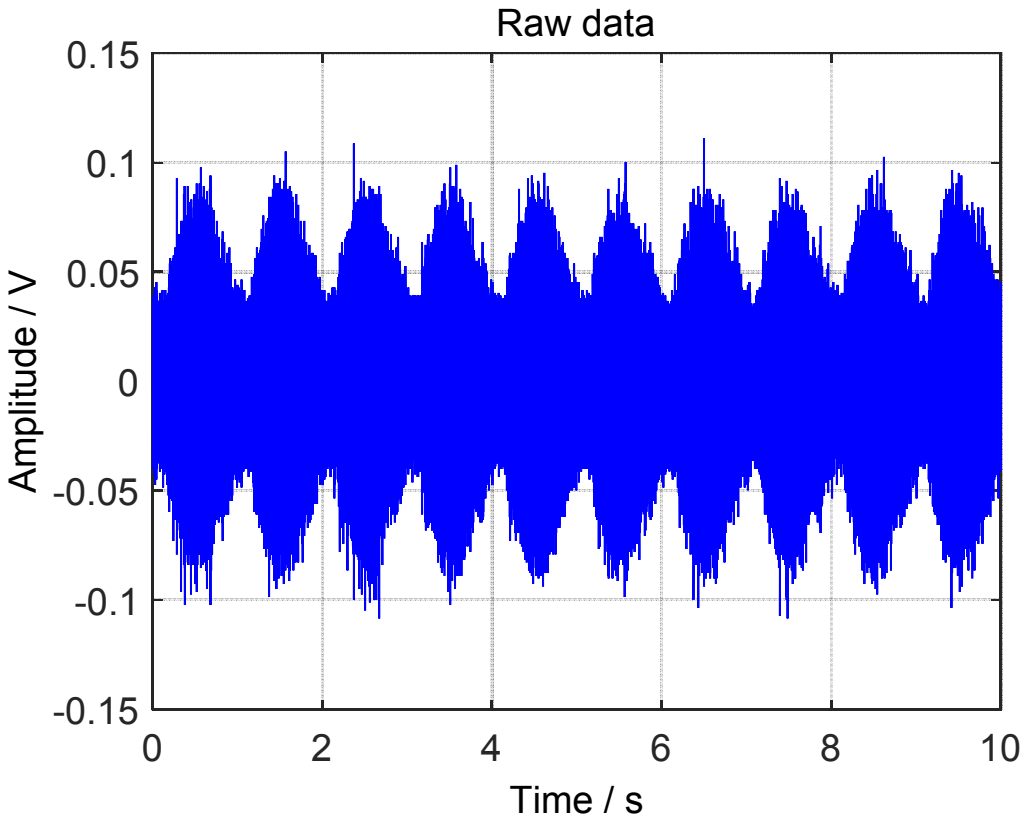

Figure 11: Raw AE signal for the reference sample within a 10-sec acquisition window. No crack growth event occurs.

Figure 12 shows the plot of SK of the raw AE signal shown in figure 11. SK values are low particularly at higher frequency range. At the lower frequency range the peaks observed are attributed to mechanical noise from the machine.

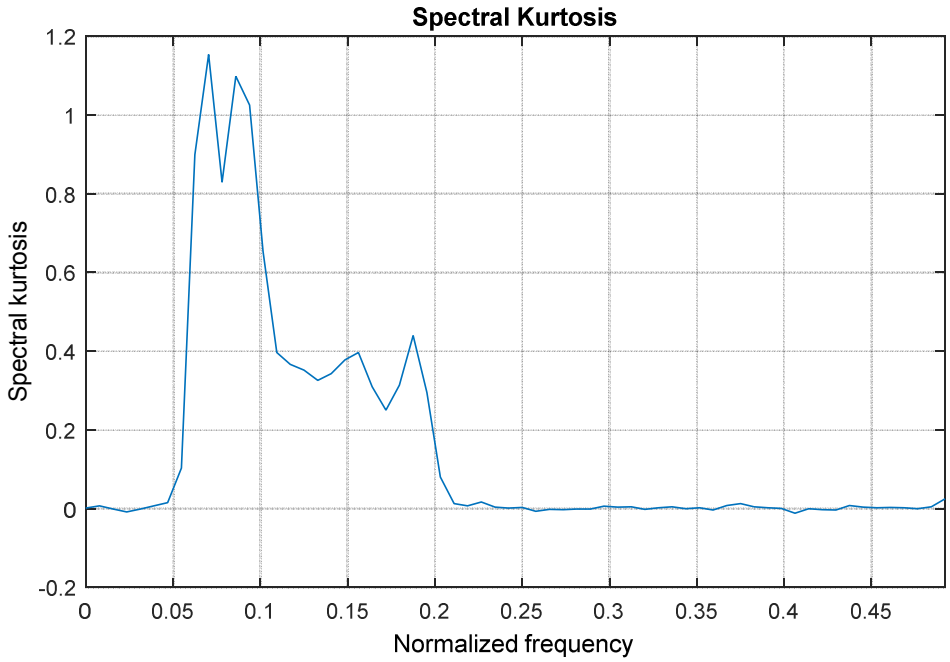

Figure 11: SK versus normalized frequency for the reference sample

Figure 12 shows the raw AE signal from pre-cracked R260 rail steel sample recorded with the customised AE system at the early stage of the fatigue test. Clear peaks related to crack growth event can be seen and the maximum amplitude reaches around 0.5V.

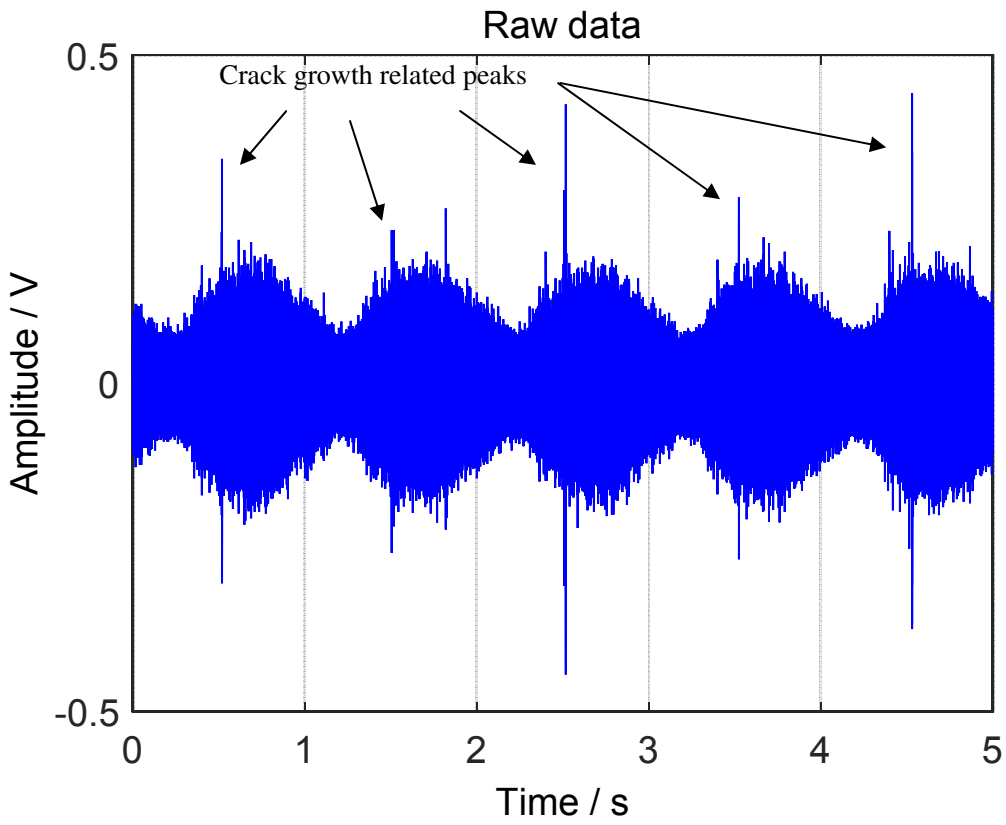

Figure 12: Raw AE data obtained during testing of a pre-cracked R260 rail steel sample during a 5s acquisition window. Peaks seen are related to crack growth events.

Figure 13 shows the SK plot for the above raw AE signal. It is clearly seen that the peaks have shifted towards higher frequencies and maximum peak value has increased considerably. As crack growth rate increases peak-peak values and SK values are expected to also increase.

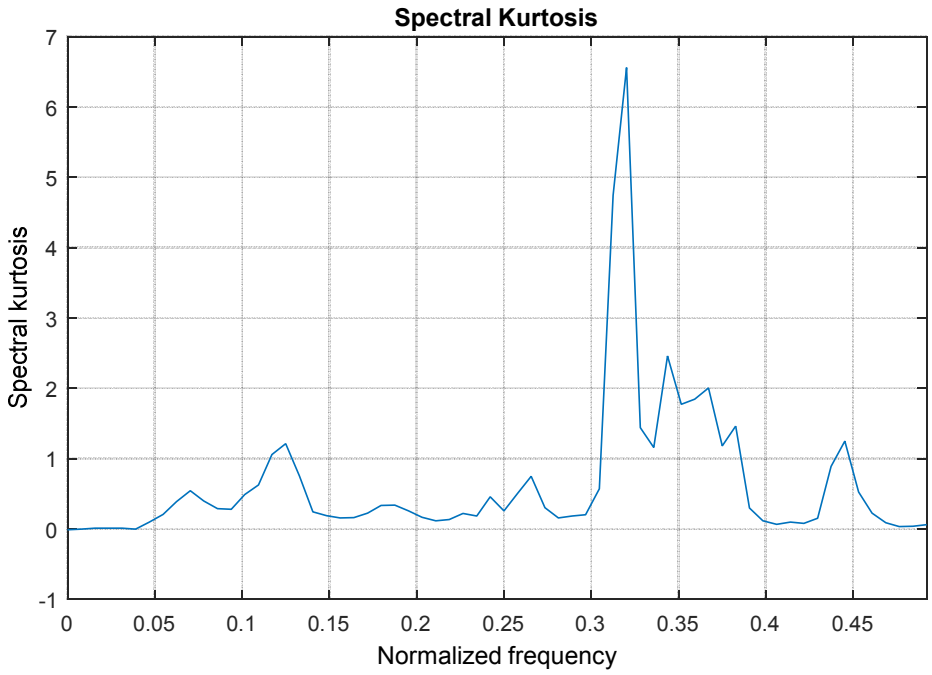

Figure 13: SK versus normalized frequency for the same sample.

Figure 14 shows the raw AE data for the same sample at a later stage where crack length has increased further. The amplitude of the crack growth related signal peaks has intensified during certain loading cycles in comparison with the previous plot. However, what is also interesting is that peaks of significant amplitude arise during the unloading part of the signal. This is attributed to the rubbing of the two facets of the fatigue crack as it unloads giving rise to AE peaks with significant amplitude in some cases. Rubbing of crack facets is an AE source which can be filtered out either by using appropriate parameter thresholds (e.g. minimum amplitude, duration, etc.) as well as higher frequency filters not present in the customised acquisition system. The nature of the source of these peaks is also further ascertained in the SK plot shown in figure 15 where the highest peak is present at a lower frequency range (around 120 kHz).

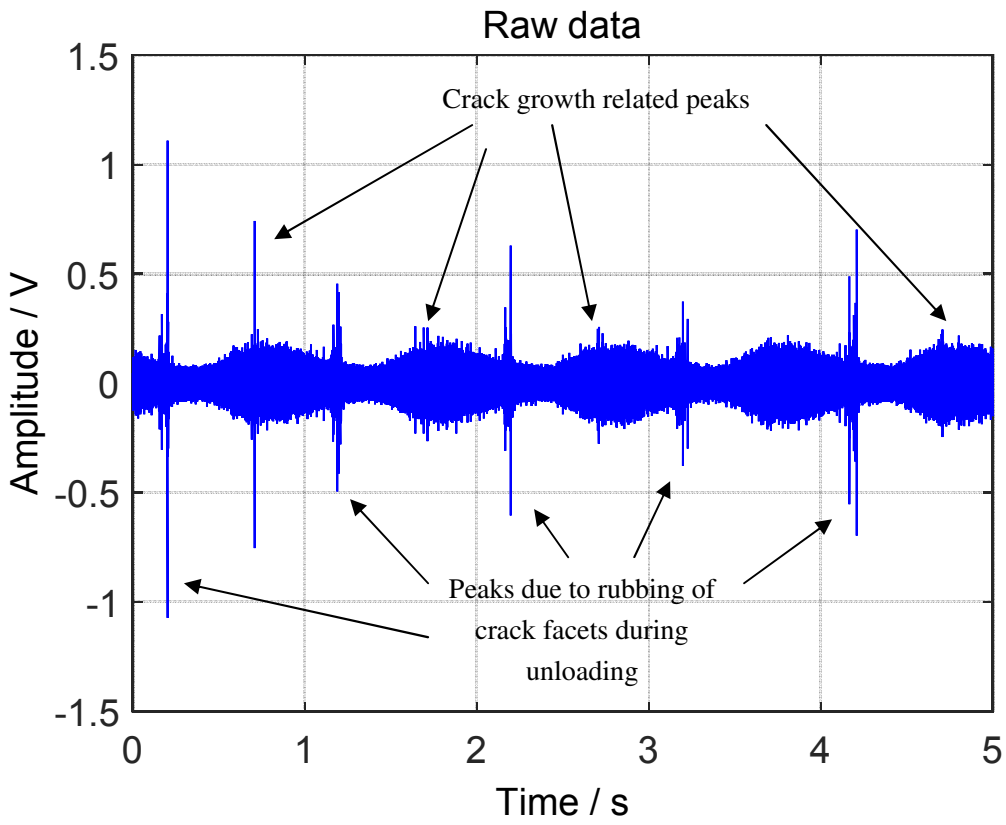

Figure 14: Raw AE data for the R260 rail steel sample at a later stage showing higher amplitude peak-peak values during crack growth.

The resulting SK peaks exhibit higher amplitudes but vary further with frequency in comparison with the previous plot as seen from figure 15. This is due to the more intense effect of mechanical noise generated by the rubbing of the crack facets as the crack opens and closes during each loading and unloading cycle. Crack growth is still occurring but the amplitude of the crack growth related events varies considerably.

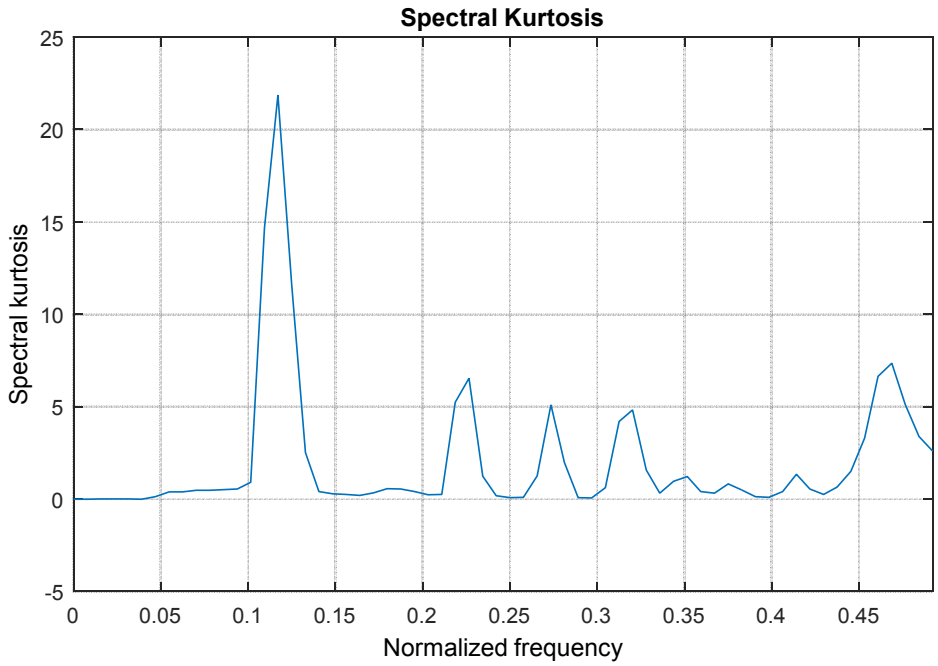

Figure 15: SK versus normalised frequency for above raw AE signal showing higher amplitude peaks but also increased variability over frequency range due to the effect from the mechanical noise arising from the rubbing of the crack facets.

8 Conclusions and future work

From the results obtained it has been clearly shown that AE can be applied for monitoring crack growth in rails. Two different loading frequencies have been considered each posing different challenges in terms of filtering background mechanical noise associated with the fatigue testing machines. As a result different filtering strategies have been employed together with two different sets of sensors. From the results obtained, although it is obvious that all samples largely obey the Paris-Erdogan law, dE/dN with respect to ΔK shows noticeable variability. This makes difficult the prediction of the remaining fatigue lifetime of rail steel using AE data alone. Nonetheless, it has also been shown that dD/dN is a plausible alternative

parameter to dE/dN producing similar trends when plotted versus ΔK.

The AE energy and fractograph results showed that brittle fracture occurred intermittently and at some certain crack lengths during fatigue crack growth for all specimens. The AE data were clearly related to the microstructural features associated with cleavage fracture events in the case of the fourth sample. This is a clear indication that brittle fracture can be quantitatively characterised using AE energy.

In addition, complete AE waveform acquisition has been attempted for short interrupted data acquisition intervals lasting for 5s. Signal processing has been conducted based on SK. Although both peak-peak and SK values change in line with damage progression, SK results show strong variability. This is due to the effect arising from the mechanical noise cause by the rubbing of the facets of the crack as it opens and closes during loading and unloading.

Based on the raw AE data obtained, time domain signal processing based on moving RMS, Crest Factor and Kurtosis can produce reasonably good results. However, care needs to be given in filtering out the peaks arising from background mechanical noise prior to using time domain-based algorithms. Although the application of SK is challenging it is worth investigating its applicability in more depth along with other algorithms including FFT, wavelet analysis, etc.

Although prediction of the remaining lifetime of defective challenges using AE data alone is by no means straightforward, it seems that using AE energy and duration rates can provide a meaningful indicator in evaluating the criticality of monitored cracks. Therefore, these two parameters can be effectively correlated with the structural degradation in a dynamic manner. Some short-term predictive capacity is also possible in this way. However, long-term prediction of the remaining lifetime is still risky considering also the stochastic nature of loading patterns sustained by rails which add further to the complexity of the problem.

Further work is planned to be undertaken under actual operational conditions and under more noisy environments in order to evaluate the feasibility of applying AE RCM in the field. Alternative signal processing methodologies combined with FE simulation and fatigue models will also be considered as part of this work.

Acknowledgements

The authors would like to thank Network Rail for the support received with respect to this work. Mr S. Shi would also like to express his gratitude for the scholarship provided from the National Structural Integrity Research Centre, the Birmingham Centre for Railway Research and Education and the School of Metallurgy and Materials at the University of Birmingham. The authors are also indebted to Dr Timothy Doel and Mr David Price at the School of Metallurgy and Materials of the University of Birmingham for their valuable assistance during fatigue testing.

References

[1] M. Papaelias, C. Roberts, C. Davis, A review on non-destructive evaluation of rails: State-of-the-art and future development, Proceedings of the IMechE: Part F – Journal of Rail and Rapid Transit, 222, 4, pp. 367-384.

[2] R. Clark, Rail flaw detection: overview and needs for future developments, NDT & E International, 2004, 37, pp. 111-118.

[3] M. Papaelias, Chapter 2: An integrated strategy for efficient non-destructive evaluation of rails, Fault Detection: Classification, Techniques and Role in Industrial Systems, Fausto Pedro Garcia Marquez and Mayorkinos Papaelias (Eds.), Nova Science Publishers, 2013.

[4] J. Peng, G. Y. Tian, L. Wang, X. Gao, Y. Zhang, Z. Wang, Rolling contact fatigue detection using eddy current pulsed thermography, 2014 IEEE Far East Forum on Nondestructive Evaluation/ Testing (FENDT), Chengdu, China, 20-23 June 2014.

[5] R. Yang, Y. He, B. Gao, G. Y. Tian, J. Peng, Lateral heat conduction based eddy current thermography for detection of parallel cracks and rail tread oblique cracks, Measurement, Vol. 66, April 2015, pp. 54-61.

[6] J. Peng, G. Y. Tian, L. Wang, Y. Zhang, K. Li, X. Gao, Investigation into eddy current pulsed thermography for rolling contact fatigue detection and characterization, NDT & E International, Vol. 74, September 2015, pp. 72-80.

[7] M. Papaelias, F. P. G. Marquez, J. M. C. Munoz, C. Roberts, A B-spline approach to alternating current field measurement for railroad inspection, IEEE International

Conference on Industrial Engineering and Engineering Management, IEEM 2008, 8-11 December 2008, Singapore, pp. 1385-1389.

[8] M. Papaelias, C. Roberts, C. L. Davis, B. Blakeley, M. Lugg, High-speed inspection of rolling contact fatigue in rails using ACFM sensors, Insight – Non-Destructive Testing and Condition Monitoring, Vol. 51, Issue 7, 2009, pp. 366-369.

[9] M. Papaelias, M. Lugg, C. Roberts, C. Davis, High-speed inspection of rails using ACFM techniques, NDT & E International, Vol. 42, Issue 4, 2009, pp. 328-335.

[10] M. Papaelias, C. Roberts, C. L. Davis, B. Blakeley, M. Lugg, Further developments in high-speed detection of rail rolling contact fatigue using ACFM techniques, Insight – Non-Destructive Testing and Condition Monitoring, Vol. 52, Issue 7, 2010, pp. 358-360.

[11] M. Papaelias and M. Lugg, Detection and evaluation of rail surface defects using alternating current field measurement techniques, Proceedings of the Institution of Mechanical Engineers Part F: Journal of Rail and Rapid Transit, Vol. 226, Issue 5, 2012, pp. 530-541.

[12] J. M. C. Munoz, F. P. G. Marquez, M. Papaelias, Railroad inspection based on ACFM employing a non-uniform B-spline approach, Mechanical Systems and Signal Processing, Vol. 40, Issue 2, 2012, pp. 605-617.

[13] J. Al-Dalabeeh, C. Roberts, M. Papaelias, Analysis of alternating current field measurement rail inspection signals, 51st Annual Conference of the British Non-Destructive Testing, NDT 2012, Daventry, UK, 11-13 September 2012.

[14] R. S. Edwards, C. Holmes, Y. Fan, M. Papaelias, S. Dixon, C. L. Davis, B. W. Drinkwater, C. Roberts, Ultrasonic detection of surface-breaking railhead defects, Insight – Non-Destructive Testing and Condition Monitoring, Vol. 50, Issue 7, 2009, pp. 369-373.

[15] H. Rowshandel, M. Papaelias, C. Roberts, C. Davis, Development of autonomous ACFM rail inspection techniques, Insight-Non Destructive Testing and Condition Monitoring, Vol. 53, Issue 2, 2011, pp. 85-89.

[16] G. Nicholson, A. Kostryzhev, H. Rowshandel, M. Papaelias, C. Davis, C. Roberts, Sizing and tomography of rolling contact fatigue cracks in rails using NDT technology – potential for high speed application, 9th World Congress on Railway Research, Lille, France, 2011.

[17] Industrial Standard (Network Rail) NR/L2/TRK/001/Mod07: Inspection and mamaintenance of permanent way: Management of rail defects, 1/12/2012.

[18] C. Turner, et al., A review of key planning and scheduling in the rail industry in Europe and UK. Proceedings of the Institution of Mechanical Engineers, Part F: Journal of Rail and Rapid Transit, 2015: p. 0954409714565654.

[19] P. Yılmazer, A. Amini and M. Papaelias, The structural health condition monitoring of rail steel using acoustic emission techniques, In the Proceedings of NDT 2012 Conference, BINDT, UK, September, 2012.

[20] N. Dadashi, et al. A framework of data processing for decision making in railway intelligent infrastructure, In the proceedings of IEEE First International Multi-Disciplinary Conference in Cognitive Methods in Situation Awareness and

Decision Support (CogSIMA), 2011.

[21] D. O. Harris and H. L. Dunegan, Continuous Monitoring of Fatigue Crack Growth by Acoustic Emission Techniques, Experimental Mechanics, Third SESA International Congress on Experimental Mechanics, Los Angeles, California, U.S.A., 13-18 May 1973, pp. 71-81.

[22] Avraham Berkovits and Daining Fan, Study of fatigue crack characteristic by acoustic emission. Eng. Fract. Mech. 51, 1995, pp. 401-416.

[23] T. M. Roberts and M. Talebzadeh, Acoustic emission monitoring of fatigue crack propagation, J. Constr. Steel. Res. 59, 2003, pp. 695–712.

[24] T. M. Roberts and M. Talebzadeh, Fatigue life prediction based on crack propagation and acoustic emission count rates, J. Constr. Steel. Res. 59, 2003, pp. 679–694.

[25] M. N. Bassim, S. ST. Lawrence and C. D. Liu, Detection of the onset of fatigue crack growth in rail steels using acoustic emission, Engineering Fracture Mechanics 41, 1994, pp. 207-214.

[26] P. Yilmazer, Structural health condition monitoring of rails using acoustic emission techniques, M.Res. Thesis, University of Birmingham, Birmingham, UK 2012.

[27] Z. Han et al., Acoustic Emission Monitoring of Brittle Fatigue Crack Growth in Railway Steel, WCAE 2015, Hawaii, USA, November 2015.

[28] D. F. Cannon, K-). Edel, S. L. Grassie, K. Sawley, Rail defects: an overview, Fatigue Fract. Engng Mater. Struct., 2003, 26, pp. 865-887.

[29] S. L. Grassie, Rolling Contact Fatigue on the British railway system: treatment, Wear, 2005, 258, pp. 1310-1318.

[30] S. L. Grassie, Squats and squat-type defects in rails: the understanding to date. Proceedings of the Institution of Mechanical Engineers, Part F: Journal of Rail and Rapid Transit, 226, 3, 2012, pp. 235-242.

[31] A. A. Pollock, Back to basics, Loading and stress in acoustic emission testing, American Society for Nondestructive Testing, March 2004.

[32] R. F. Dwyer, Detection of non-Gaussian signals by frequency domain kurtosis estimation, In Proceedings of IEEE International Conference of Acoustics, Speech, and Signal Processing, 1983.

[33] C. Ottonello and S. Pagnan, Modified frequency domain kurtosis for signal processing. Electronics Letters, 30, 14, 1994, pp. 1117-1118.

[34] S. Pagnan, C. Ottonello, and G. Tacconi, Filtering of randomly occurring signals by kurtosis in the frequency domain, In Proceedings of the IEEE 12th IAPR International Conference on Pattern Recognition, Vol. 3: Signal Processing, 1994.

[35] J. Antoni, The spectral kurtosis: a useful tool for characterising non-stationary signals, Journal of Mechanical Systems and Signal Processing, 20, 2, 2006, pp. 282-307.

[36] Industrial Standard BS EN 13674-1:2011 - Railway applications. Track. Rail. Vignole railway rails 46 kg/m and above, Published February 2011.

[37] S. Suresh, Fatigue of Materials, Cambridge University Press, 1991.

[38] J. Yu, P. Ziehl, B. Zárate, J. Caicedo, Prediction of fatigue crack growth in steel

bridge components using acoustic emission, J. Constr. Steel. Res. 67, 2011, pp. 1254-1260.

[39] E.T. Ng, G. Qi. Material fatigue behavior characterization using the wavelet-based AE technique – a case study of acrylic bone cement, Engineering Fracture Mechanics, 68, 2001, pp. 1477-1492.